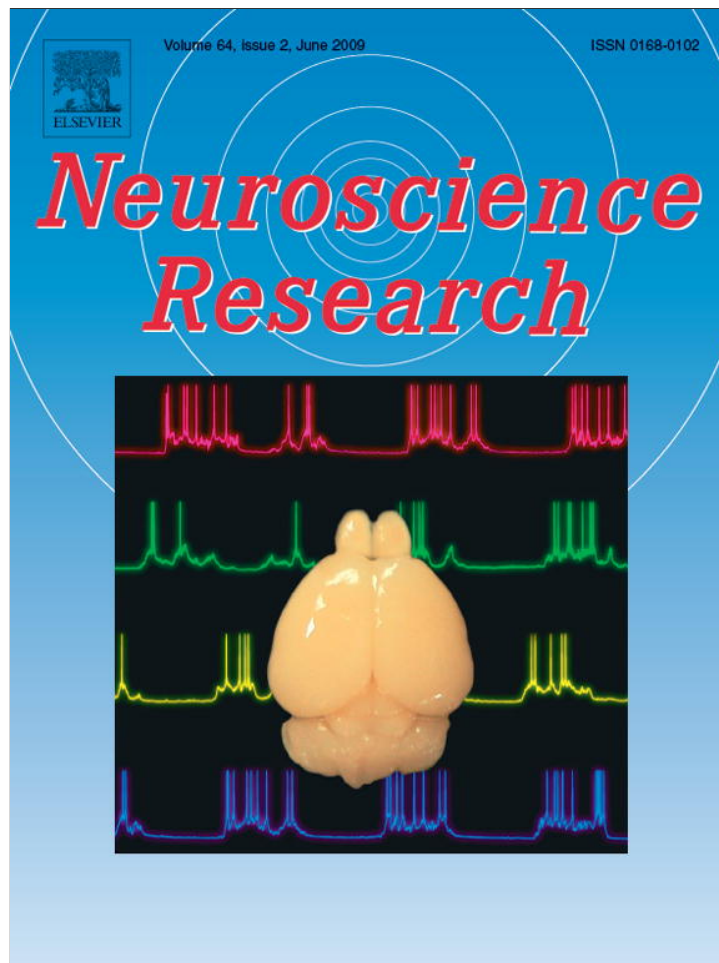


Provided for non-commercial research and education use.
Not for reproduction, distribution or commercial use.



This article appeared in a journal published by Elsevier. The attached copy is furnished to the author for internal non-commercial research and education use, including for instruction at the authors institution and sharing with colleagues.

Other uses, including reproduction and distribution, or selling or licensing copies, or posting to personal, institutional or third party websites are prohibited.

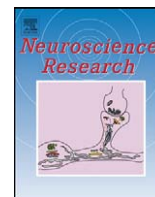
In most cases authors are permitted to post their version of the article (e.g. in Word or Tex form) to their personal website or institutional repository. Authors requiring further information regarding Elsevier's archiving and manuscript policies are encouraged to visit:

<http://www.elsevier.com/copyright>



Contents lists available at ScienceDirect

Neuroscience Research

journal homepage: www.elsevier.com/locate/neures

Analysis of ongoing dynamics in neural networks

Toru Yanagawa^{a,b}, Ken Mogi^{a,b,*}

^a Sony Computer Science Laboratories, Takanawa Muse Bldg., 3-14-13, Higashigotanda, Shinagawa-ku, Tokyo, 144-0022, Japan

^b Department of Computational Intelligence and System Science, Interdisciplinary Graduate School of Science and Engineering, Tokyo Institute of Technology, 4259 Nagatsuta-cho, Midori-ku, Yokohama, 226-8503, Japan

ARTICLE INFO

Article history:

Received 28 January 2008
 Received in revised form 19 February 2009
 Accepted 24 February 2009
 Available online 9 March 2009

Keywords:

Hodgkin–Huxley equation
 Excitatory–inhibitory network
 Mexican-hat interaction
 Ongoing activity
 Synaptic depression
 Depolarization-dependent potassium channels

ABSTRACT

Spontaneous neural activities in the cerebral cortex exhibit complex spatio-temporal patterns in the absence of sensory inputs [Arieli, A., Shoham, D., Hildesheim, R., Grinvald, A., 1995. Coherent spatio-temporal patterns of ongoing activity revealed by real-time optical imaging coupled with single-unit recording in the cat visual cortex. *J. Neurophysiol.* 73, 2072–2093; Arieli, A., Sterkin, A., Grinvald, A., Aertsen, A., 1996. Dynamics of ongoing activity: explanation of the large variability in evoked cortical responses. *Science* 273, 1868–1871], wandering among the intrinsic set of cortical states [Tsodyks, M., Kenet, T., Grinvald, A., Arieli, A., 1999. Linking spontaneous activity of single cortical neurons and the underlying functional architecture. *Science* 286, 1943–1946; Kenet, T., Bibitchkov, D., Tsodyks, M., Grinvald, A., Arieli, A., 2003. Spontaneously emerging cortical representations of visual attributes. *Nature* 425, 954–956]. Elucidating the nature of such spontaneous activities is one of the most intriguing challenges in the effort to understand the computational principles employed by the brain. The precise mechanism behind these salient phenomena, however, is not known. Here we model the ongoing dynamics of generic neural networks with attractor states using a conductance-based neuron model. Our realistic modeling shows the existence of up-states and down-states in the membrane potential, where the up-states exist as spatially clustered patches moving within the network. Our analysis shows that up-states are sustained by the balance between excitatory and inhibitory inputs. Synaptic depression and depolarization-dependent potassium channels can cause the transitions from the up-states to down-states by affecting the dynamics in differential manners. The velocity of patches depends on the firing frequency of excitatory neurons affected by contributing factors. These results suggest that the switching dynamics can be produced by the interactions within the local network, revealing the constraints on the nature of autonomous dynamics within the cortex.

© 2009 Published by Elsevier Ireland Ltd and the Japan Neuroscience Society.

1. Introduction

The cortical circuit is activated spontaneously even when there is no or little sensory input. From the empirical point of view, spontaneous neural activities (Arieli et al., 1995, 1996; Tsodyks et al., 1999; Kenet et al., 2003) and behaviors (Maye et al., 2007) represent the most salient and interesting differences between the biological brain and the artificial computer, supporting flexible and dynamic perception of the environment. On the larger cortical scale, the existence of the “default” system has been suggested to play an important role in the functionality of the brain, in which

baseline activities are sustained by specific cortical areas (Raichle et al., 2001; Vincent et al., 2007). At the scale of local networks, the “ongoing activities” exhibit complex spatio-temporal patterns that switch between a set of intrinsic cortical states (Tsodyks et al., 1999), reflecting the overall cortical architecture. Kenet et al. (2003) observed the ongoing activities in the visual cortex of anesthetized cats using voltage-dependent optical imaging and found that the ongoing activities went through cortical states coincident with orientation columns.

There are two possible basic mechanisms underlying the ongoing activities and their transitions (Goldberg et al., 2004). The first assumes that the ongoing activities are driven by cortical noise and are merely the manifestations of the dynamics of a single external background state (single-state hypothesis). The second assumes that the ongoing activities reflect the specifics of internal cortical interaction, with the cortical state wandering through a series of intrinsic states as a result (attractor-state hypothesis).

* Corresponding author at: Sony Computer Science Laboratories, Fundamental Research Lab, Takanawa Muse Bldg., 3-14-13, Higashigotanda, Shinagawa-ku, Tokyo, 144-0022, Japan. Tel.: +81 3 5448 4380; fax: +81 3 5448 4273.

E-mail address: kenmogi@qualia-manifesto.com (K. Mogi).

Theoretical studies show that there is a trade-off between mechanisms that support the single-state hypothesis and those that support the attractor-state hypothesis. In the case of the single-state hypothesis, the ongoing activities are driven by cortical noise external to the network in question. The membrane potentials of neurons in the simulation rise transiently by the noise, and fall according to the decay time constant of the membrane potential, characterized by a fast transition (<100 ms). The correlation of membrane potential over space tends to be small, since the interactions within the local cortical network are weak. Cai et al. (2005) constructed a large-scale neural network of the visual cortex. They controlled the coupling strength of long-range connection and reproduced the ongoing activities with transient strong spatial correlation. They suggested that the ongoing activities in visual cortex could be accounted for by mechanisms other than those based on the attractor-state hypothesis. Specifically, they introduced the scenario of an intermittent desuppressed state (IDS), which is a dynamic state of high conductance, strong inhibition, and large fluctuations that arise from intermittent spiking events that are strongly correlated in time as well as in orientation domains, with the correlation time of the fluctuations controlled by the NMDA decay time scale. In the case of attractor hypothesis, on the other hand, the ongoing activities are sustained by recurrent inputs within the network, where the spatial correlation of membrane potential tends to be large. In a system characterized by the attractor hypothesis, the time scale of transition tends to be long (>100 ms), due to the time required to break the stability of the up-state.

Spontaneous neural activities involving the up-states and the down-states are ubiquitously found in the biological brain. During the naturally occurring slow wave sleep (SWS) in non-anesthetized cats, there are oscillations (<1 Hz) between the depolarized and hyperpolarized phases. In the up-states, neural activities are sustained by strong recurrent excitation balanced by the inhibition involving some intrinsic channels. In the down-states, a majority of cortical neurons are hyperpolarized, possibly caused by the synaptic depression and the depolarization-dependent potassium channels (Compte et al., 2003; Bazhenov et al., 2002; Hill and Tononi, 2005). Depolarization-dependent potassium channels have been shown to be essential in reproducing the down-states (Compte et al., 2003; Hill and Tononi, 2005).

Incorporating the up-states and down-states as significant ingredients is compatible with the attractor-state hypothesis in which the up-states could be sustained by recurrent cortical interactions. Such a model needs to reproduce two properties of spontaneous activities. The first is that the neural activities have patch-like spatial correlation, reflecting the cortical architecture. The second is that the neural activities exhibit transient changes, characterized by time scales corresponding to the physiological data.

Here we hypothesized that the switching between the cortical states of spontaneous ongoing activities in visual cortex is the result of the transition dynamics between the up-states and down-states. We investigate the transitions within the ongoing dynamics in a generic network by combining the biophysical neuron model with the Mexican-hat type interaction (i.e., excitation dominating on the short spatial range followed by inhibition on the longer range), incorporating synaptic depression and depolarization-dependent potassium channels. In the local circuitry of primary visual cortex (V1), the Mexican-hat type interaction causes recurrent interaction leading to cortical states selective to orientations (Ben-Yishai et al., 1995; Ernst et al., 2001). The synaptic depression and the depolarization-dependent potassium channel cause the transitions from the up-states to the down-states. Our simulation shows that the transition velocity of ongoing activities in the visual cortex can be reproduced by adjusting the

parameters of synaptic depression and depolarization-dependent potassium channels, despite the general tendency of slow transitions in neural network models based on the attractor-state hypothesis. The necessary fine-tuning of parameters involved puts considerable constraints on the makeup of the network. We discuss the differential effects of synaptic depression and depolarization-dependent potassium channels on the ongoing activities. The velocities of traveling waves are rate-limited by the transition from the up-state to the down-state, contrary to previous models (Compte et al., 2003; Bazhenov et al., 2002; Golomb and Ermentrout, 2001, 2002) in which the transition from the down-state to the up-state is rate-limiting. Finally, we suggest to test the relevance of mechanisms based on the attractor-state hypothesis for biological networks such as the primary visual cortex by adjusting the parameters of synaptic depression and depolarization-dependent potassium channels.

2. Methods

We used Hodgkin–Huxley equations similar to those described by Compte et al. (2003). The pyramidal neurons were modeled as consisting of two compartments, the soma and the dendrite. The spiking currents I_{Na} and I_K were located in the soma, together with a leak current I_L , a fast A-type K^+ current I_A , a non-inactivating slow K^+ current I_{KS} and a depolarization-dependent potassium current I_{KNa} . The dendrite contained a high threshold Ca^{2+} current I_{Ca} , a Ca^{2+} -dependent K^+ current I_{KCa} , a non-inactivating (persistent) Na^+ current I_{NaP} , an inward rectifier (activated by hyperpolarization) non-inactivating K^+ current I_{AR} . The depolarization-dependent potassium channel appears to cause the termination of the depolarized phase of the slow oscillation (Sanchez-Vives and McCormick, 2000). This channel is activated by the influx of sodium ion that accumulate during the period of depolarization and spiking.

Interneurons consisted of a single compartment, with spiking currents I_{Na} and I_K , and a leak current I_L . These parameters were given explicit treatment within the dynamics described by the equations.

Excitatory synaptic current consisted of an AMPA-mediated current and an NMDA-mediated current (Jahr and Stevens, 1990; Wang, 1999). Inhibitory synaptic current was modeled as a GABA-mediated current (Wang, 1999). A short-term synaptic depression was introduced for pyramidal-to-pyramidal recurrent excitatory connections (Tsodyks and Markram, 1997; Abbott et al., 1997). The synaptic depression reduces the synaptic current in response to the contiguous spikes of presynaptic neurons and recovers it in the absence of presynaptic activities.

The initial values for membrane potentials were randomly distributed around the mean values of -50 mV and -60 mV for the excitatory and inhibitory neurons, respectively, with a range of ± 10 mV. No delay was explicitly assumed in the transmission between the neurons.

For further details about the models used in the simulation, refer to the [supplementary material \(Text S1\)](#).

The generic network consisted of 2304 pyramidal neurons and 576 interneurons. The pyramidal neurons were arranged on a regular square grid (Fig. 1(c)). Inhibitory neurons were positioned on every second grid points, half a grid out of alignment from excitatory neurons. The network had a periodic boundary condition, leading to a 2D torus topology. The excitatory and inhibitory synaptic connections were given by a Gaussian distribution. Following previous works (Ben-Yishai et al., 1995; Ernst et al., 2001; Crook et al., 1998), we assumed that the excitatory and inhibitory synaptic connections induce lateral interactions having a Mexican-hat type shape. Standard deviation of the Gaussian was set to be 2 grids and 4 grids for the excitatory

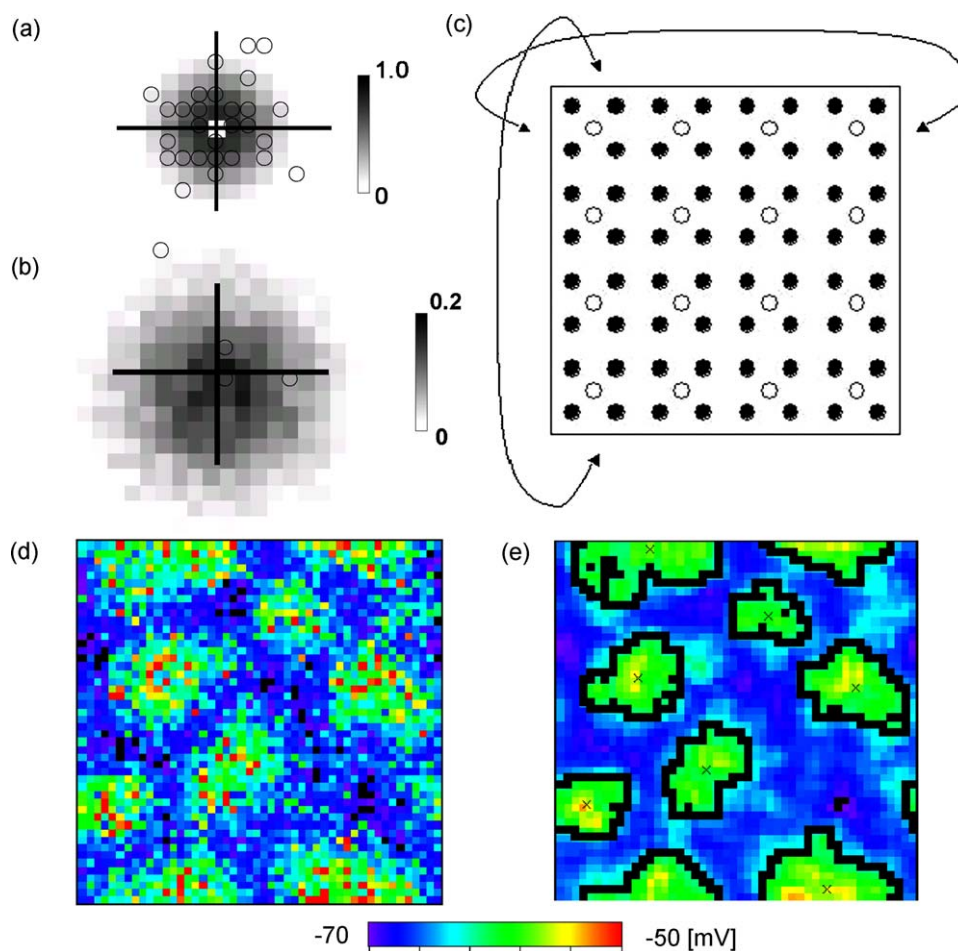


Fig. 1. (a) Distribution of presynaptic excitatory neurons as “seen” from an excitatory neuron. Gray scales represent the average distribution of excitatory neurons. The scale bar represents the probability values between 0 and 1.0. Open circles represent the typical actual distribution of excitatory neurons. (b) Presynaptic inhibitory neurons “seen” from an excitatory neuron. Gray scales represent the average distribution of inhibitory neurons. The scale bar represents the probability values between 0 and 0.2. Open circles represent the typical actual distribution of inhibitory neurons. (c) The network architecture. Filled circles represent the excitatory neurons. The open circles represent the inhibitory neurons. (d) A snapshot of the membrane potentials of the soma in the excitatory neurons. (e) A snapshot of the membrane potentials of the soma in the excitatory neurons after spatial interpolation. The black lines represent the borders between up-states and down-states. The centroids of the patches are represented by the symbols “x”.

(σ_{ex}) and inhibitory (σ_{inh}) synapses, respectively. The number of presynaptic neurons was set to be constant. For pyramidal and inhibitory neurons, the number of presynaptic excitatory neurons was 28, while that for presynaptic inhibitory neurons was 4. As a result of the assignment process following the Gaussian distribution constrained by the fixed number of presynaptic neurons, the number of postsynaptic neurons had some degrees of variance in the process of random selection for the target neurons. For the pyramidal neuron, the number of post-synaptic pyramidal neurons was 28 ± 3 while that for inhibitory neurons was 7 ± 1.7 . For the inhibitory neuron, the number of post-synaptic pyramidal neuron was 16 ± 2.9 and that of inhibitory neurons was 4 ± 1.9 .

The model was implemented in a C++ code and simulated using a forth-order Runge-Kutta method with a time step of 0.06 ms.

3. Results

The synaptic depression and the depolarization-dependent potassium channels are two possible candidates for the mechanism that causes the transition from the up-state to the down-state. The activation of depolarization-dependent potassium channel results in the hyperpolarization of excitatory neurons (Compte et al., 2003; Hill and Tononi, 2005). Therefore we tested two conditions. Firstly, we simulated the network with the synaptic

depression only (condition1). Secondly, the depolarization-dependent potassium channel was introduced to the network in addition to the synaptic depression (condition 2).

First we describe the simulation based on condition 1. Since the reversal potential and peak conductance of the leakage current is distributed randomly (see Text S1), some pyramidal neurons are spontaneously active with low firing rates (0.2 ± 0.4 Hz). This arrangement is based on the observation of spontaneously firing activities even after blocking the glutamatergic excitatory postsynaptic potentials in *in vitro* experiments (Sanchez-Vives and McCormick, 2000). This is the only source of spontaneous activity in this simulation.

In condition 1, when a random initial condition was given, spontaneously active neurons fired together occasionally, which triggered a cascade of recurrent excitation that locally brought the network into the firing regime of the up-states (see Text S5). The local Mexican-hat type interaction between excitatory and inhibitory neurons generated a spatially heterogeneous (patchy) distribution (Fig. 2(g)). After the network went into the steady state, the patches of up-states started to move (Video S16, http://www.qualia-manifesto.com/Video_S16.mov). The membrane potential showed a robust oscillation (see Text S10). The distribution of the histogram of the membrane potential of excitatory neurons in the steady state remained essentially

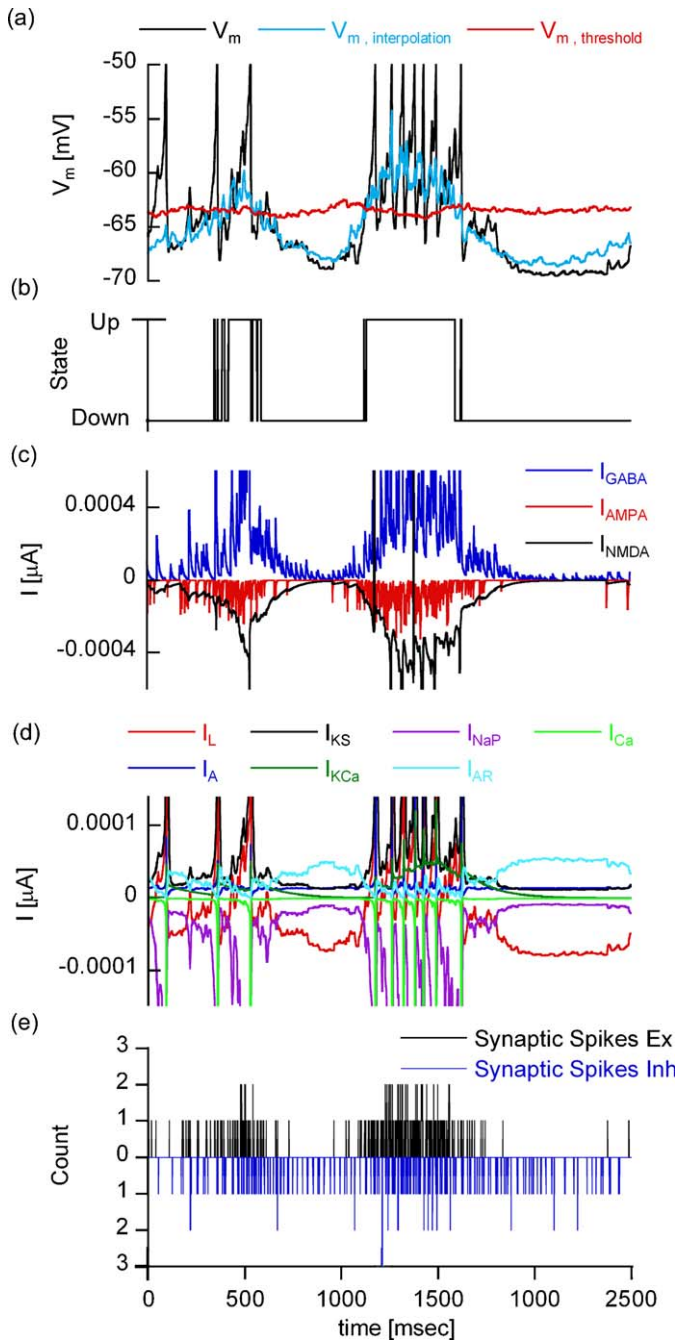


Fig. 2. (a) The membrane potential of a soma in the pyramidal neuron before (black trace) and after (blue trace) spatial interpolation. The threshold between the up-state and down-state is shown in the red trace. (b) A typical time course of the transition between the up-state and down-state of a neuron. (c) A typical time course of the synaptic current of GABA (blue trace), AMPA (red trace), and NMDA (black trace). (d) A typical time course of all intrinsic currents except for I_{Na} and I_K in excitatory neurons. (e) A typical count of excitatory and inhibitory synaptic spikes. (For interpretation of the references to color in this figure legend, the reader is referred to the web version of the article.)

invariant (Fig. S12). An approximately constant ratio of the population is found to be in the up-state (definition of up-state and down-state given below). In the steady state, the inhomogeneity introduced by random distribution of leakage currents is averaged by the network interaction, while the fluctuations of patch dynamics are affected by cortical interaction.

To extract and visualize the patches of activities, membrane potential of each neuron was averaged with the neighboring eight neurons (Fig. 1(e)). The Mexican-hat type interaction generated

regions of positive and negative spatial correlation (Fig. 3(b)). If we assume that the ratio (in terms of distance) of positive and negative regions is 1:1 as suggested by the data, the ratio (in terms of areas) of the positive and negative regions, each represented by concentric circles, is 1:3. As an estimate based on this result, we defined the first upper quartile of population in the distribution over the membrane potential value range as belonging to the up-state, while the remaining population was judged to be in the down-state (Fig. 2(a) and (b)). This distinction was then used for the visualization of the patches and the calculation of moving velocities for the centroids of the patches. This distinction is invariant over time (Fig. S13).

In our simulation, there are no clearly distinctive peaks in the membrane potential distributions of individual neurons (Fig. S14). Since there is no a priori reason why a particular threshold value should be adapted for the border between the up-state and the down-state, the definition above is in essence arbitrary. Notwithstanding this reservation, the dynamics of the network is found to be different for the upper and lower regions of the membrane potential, with the threshold defined above as the effective border.

The activities of the synaptic currents and intrinsic channel currents have different modes for the up-states and down-states (Fig. 2(c) and (d)). In the up-state, the AMPA-mediated, NMDA-mediated, and GABA-mediated currents are activated (Fig. 2(c)). The intrinsic channel currents, the non-inactivating slow K^+ current I_{KS} , and a non-inactivating (persistent) Na^+ current I_{NaP} , both of which are voltage-dependent channels, also get activated. In addition, the Ca^{2+} -dependent K^+ current I_{KCa} becomes open.

In the down-state, the number of excitatory synaptic inputs are smaller than that for the up-state (Fig. 2(e)). However, the inhibitory synaptic inputs are as active as in the up-state, which is caused by the Mexican-hat type interaction (Fig. 2(e)). The inward rectifier non-inactivating K^+ current I_{AR} (which is activated by hyperpolarization) is also activated.

Synaptic depression is induced in the excitatory synaptic connections between excitatory neurons. In the up-state, the excitatory synaptic current gradually decreases as the neurons keep firing, which in turn causes a decrease in the firing frequency. There exists a point where the balance between the recurrent decrease of excitatory synaptic input and the constant inhibitory synaptic input is broken (Fig. 3(a)–(i)). The term of voltage-dependence in the NMDA-mediated current, which is drastically reduced as the membrane potentials decrease, also contributes to the switching from the up-state to the down-state.

To investigate the robustness of the observed behavior of the system, we modified the following parameters: $a = (g'_{NMDA}{}^{EE} / g_{AMPA}{}^{EE}) / (g_{NMDA}{}^{EE} / g_{AMPA}{}^{EE}) = (g'_{NMDA}{}^{EI} / g_{AMPA}{}^{EI}) / (g_{NMDA}{}^{EI} / g_{AMPA}{}^{EI})$, which changes the strength of NMDA-mediated current, and $b = g'_{AMPA}{}^{EI} / g_{AMPA}{}^{EI}$ which affects the strength of inhibitory feedback. In all conditions, $g_{AMPA}{}^{EE}$ was kept constant. Namely, $g'_{NMDA}{}^{EE} = a g_{NMDA}{}^{EE}$, $g'_{AMPA}{}^{EI} = b g_{AMPA}{}^{EI}$, and $g'_{NMDA}{}^{EI} = a b g_{NMDA}{}^{EI}$.

As a measure of the heterogeneity between the up-states and the down-states, the spatial correlation coefficients between the membrane potentials of excitatory neurons were calculated. The spatial correlation for the patches of up-state is found to depend on the strength of NMDA-mediated current (Fig. 3(b) and (c)).

The parameter b controlled the strength of the inhibitory feedback. When b was large, the strength of inhibitory feedback became correspondingly large, and the spatial correlations decreased (Fig. 3(c)). On the other hand, when the inhibitory feedback became smaller, the network came close to an over-excited “epilepsy” state, with the spatial correlation becoming smaller.

The moving velocity was calculated for the trajectory of the centroid of the patches in the network (Fig. 1(e)). Here, a patch was defined as the cluster of connected up-states. The average moving

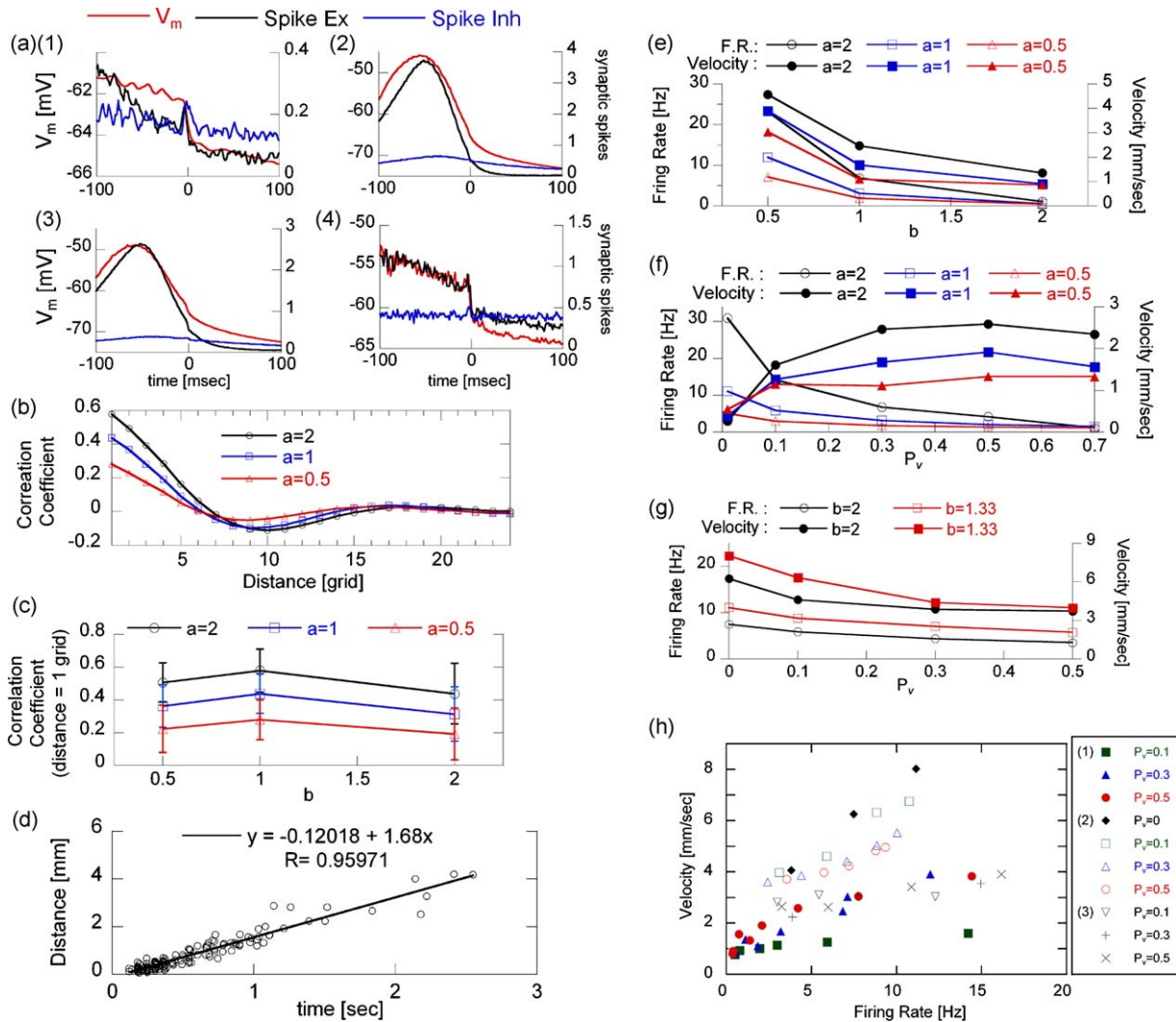


Fig. 3. (a) A typical time course of the average membrane potential of the soma of excitatory neurons and the average count of synaptic excitatory and inhibitory spikes when the neuron goes under the transition from the up-state to the down-state. Time bin is 1.5 ms. (a-1) represents condition 1 (synaptic depression only). (a-2), (a-3), and (a-4) represent condition 2 (synaptic depression and depolarization-dependent potassium channels), with the following parameters (a-1) $a = 1, b = 1, P_v = 0.3$ (a-2) $a = 1, b = 1.33, P_v = 0$ (a-3) $a = 1, b = 0.8, P_v = 0.3$ (a-4) $a = 1, b = 1.33, P_v = 0.5$ and $I_{KNa} = 0$. These parameter values are selected so that the firing rates of excitatory neurons become ~ 10 Hz. (b) The average correlation coefficient of the membrane potential between neurons as a function of distance. Parameter $a = 0.5, 1, 2$ ($b = 1$). (c) Correlation coefficient at the distance of 1 grid for some values of parameters a and b . (d) The distance traveled as a function of the lifetime of patches with $a = 1$ and $b = 1$. The straight line depicts the result of linear regression. (e) The average firing rate of excitatory neurons and the average moving velocities for some values of parameters a and b ($P_v = 0.3$). (f) The average firing rate of excitatory neurons and the average moving velocities for some values of a and P_v ($b = 1$). (g) The average firing rate of excitatory neurons and the average moving velocities for some values of a and P_v ($a = 1$) in condition 2 (synaptic depression and depolarization-dependent potassium channels). (h) The moving velocity as a function of the average firing rate of excitatory neurons for some values of parameters a and b with $P_v = 0.1, 0.3, \text{ and } 0.5$ in condition 1 (1) and condition 2 ((2) and (3)). $I_{KNa} = 0$ in (3).

velocity of the patches was found to depend on the firing frequencies and the modes of synaptic depression. The moving patches repeatedly went through the process of generation and disappearance, while the ratio of the neural population in the up-state was roughly preserved (details described below and in the supplementary online material).

Here's a qualitative description of what is typically observed in the simulation. A patch moves continuously, being affected by and influencing in turn the motion of the surrounding patches. During its existence, the moving velocity has a certain degree of variation. When a patch is "stuck" with the surrounding patches, it slows down. Sometimes such a "traffic jam" can cause the disappearance of a patch. When a space is created in the vicinity of a patch, it "moves" for that space with an accelerated speed. There is the tendency that after the disappearance of a patch, the nearest patch splits into two patches, one of which moves for the space made vacant by the disappearance. At present, we are not aware of any

physiological data that correspond to these observed phenomena in the simulation.

Fig. 3(d) shows the relation between the lifetime of each patch and the distance traveled. A series of centroids at different times are regarded as belonging to one patch trajectory within the range of its spatio-temporal continuity. The split of a patch into two initiates a new series of trajectory. The average velocity is calculated for a single trajectory of each patch thus defined.

In our simulation, the values of parameters σ_{ex} and σ_{inh} affect the size of patches. Changing the values of σ_{ex} , σ_{inh} and the network size while keeping other parameters fixed resulted in changes of the patch sizes and their transition velocities. The transition velocity of the patches is an important parameter to be compared with the physiological data. The velocity of a patch increases linearly, following an increase of the patch size (see Supplementary data, Text S2). The dynamics on which we focused in this study do not acutely depend on the number of neurons contained in the

patch, but rather on its diameter defined by the length of σ_{ex} and σ_{inh} (Fig. S4). The patch diameter, 12 grids in our simulation, roughly corresponds to the 1 mm size of a column in the biological network (Tsodyks et al., 1999). The total size of the model network thus roughly corresponds to ~ 4 mm \times ~ 4 mm.

An increase in parameter a and a decrease in parameter b led to the increase in both the firing rate and the moving velocity (Fig. 3(e)). When the synaptic depression parameter P_v , (the rate of decrease in the current after a spike) was made larger while the firing rate was kept small, the velocity of the patch became larger (Fig. 3(f)). Fig. 3(h) shows the relation between the firing rate and the transition velocity for the patches in the parameter space. The transition velocity is observed to become faster as the firing rate and the synaptic depression parameter P_v become larger.

To the best of our knowledge, there are no physiological data explicitly addressing the traveling velocity of ongoing activities resulting from switching cortical states. Based on the available data, we estimate the traveling velocity as follows. The decay constant of autocorrelation function calculated from the time series of correlation coefficients between the evoked map and single frames from spontaneous activities is 80 ms (Kenet et al., 2003). When approximated linearly, the time in which the correlation becomes zero is 127 ms (80 ms divided by 0.63). This estimated time would be shorter than the actual time since the autocorrelation function is convex downwards. If we assume that the patch sweeps an area corresponding to a column of 1 mm in diameter, and that the cortical states would have undergone the transition from the up-state to the down-state or vice versa in that time, the traveling velocity would be 7.9 mm/s. We use this value as a rough estimate of the velocity of traveling waves *in vivo*.

In an effort to match the physiological value for the traveling velocity of the patches estimated above, we conducted further simulations with condition 2, where depolarization-dependent potassium channels were introduced in addition to synaptic depression. Along with the addition of depolarization-dependent potassium channels to the network, which enhances the inhibition effect in proportion to firing rate during the up-state, some parameters were changed from condition 1. Firstly, the permeability of the leak current I_L was reduced by decreasing the conductance and increasing the reversal potential of the leak current. This change effectively increases the influx of the potassium current during the down-state and functions to shorten the duration of the down-state, preventing the network from being in the down-state overall by the effect of I_{KNa} . Physiologically, this arrangement corresponds to the blocking of leakage currents arising from the increase of neuromodulators such as acetylcholine in the transition from the sleeping state to awake state (McCormick, 1992). Secondly, the inward rectifier non-inactivating K^+ current I_{AR} was set to be zero, as it lengthens the duration of the hyperpolarization in the down-state. The effect of I_{AR} would become otherwise stronger in the existence of I_{KNa} , forcing all neurons to the down-state. Thirdly, the conductance of non-inactivating (persistent) Na^+ current I_{NaP} was made larger, making it easier for I_{KNa} to break the balance between the excitatory and inhibitory currents.

Typical dynamics of the ongoing activity in condition 2 is shown in Fig. S18 and Movie S17 (http://www.qualia-manifesto.com/Video_S17.mov). The membrane potentials become variable in condition 2, due to the effect of depolarization-dependent potassium channels causing a strong hyperpolarization (Fig. S13 (b)). This situation makes the definition of up-state and down-state adopted for condition 1 impractical, making the border unstable in its designated properties. In condition 2 therefore, the border between the up-state and down-state was set at a constant value of membrane potential, -65 mV (Fig. S14 (b)), which was found to be effective in extracting the centroids of patches.

The decay of membrane potential in the transition from the up-state to down-state became faster when the depolarization-dependent potassium channels were incorporated (condition 2) compared to the situation with synaptic depression only (condition 1) (Fig. 3a). These results suggest that depolarization-dependent potassium channels are more effective than synaptic depression in terminating the up-states. In the presence of depolarization-dependent potassium channels, the firing rate and the velocities of the patches became smaller as the synaptic depression parameter P_v , became larger (Fig. 3(g)).

Finally, Fig. 3(h) shows that the velocities of patches are larger in the presence of synaptic depression and depolarization-dependent potassium channels than those in the presence of synaptic depression only. The firing rate was modified by manipulating the parameter b , the amplitude of inhibitory feedback to excitatory neurons. The patch velocity in the presence of depolarization-dependent potassium channels (condition 2) is closest to the physiological data (with a maximum velocity of ~ 8.0 mm/s). As parameters I_L , I_{AR} and I_{NaP} were modified along with the introduction of depolarization-dependent potassium channels in condition 2, the effect of these parameter changes alone was checked by setting the value of I_{KNa} to zero. As can be seen from Fig. 3(h), these changes in parameters by themselves cannot make the velocities comparable to the physiological level.

4. Discussion

In this study, we constructed a network of spiking neurons with up-states and down-states in the presence of synaptic depression and depolarization-dependent potassium channels. We have described some robust properties of the ongoing activities characterized by transitions between cortical states. Our study focused on the nature of the mechanism involved in the ongoing activities exhibited in, e.g., the primary visual cortex (Arieli et al., 1995, 1996; Tsodyks et al., 1999; Kenet et al., 2003).

The results reported here describe the properties of a generic neural network. The architecture in our model has an isotropic local connectivity which follows a Gaussian distribution. Several evidences suggest that such a rudimentary architecture can actually be regarded as a founding basis for the biological neural network. Although functional maps are organized at a fine scale in the primary visual cortex (V1) (Tsodyks et al., 1999), it is known that cortical neurons have isotropic local connectivity even at the pinwheel centers (Marino et al., 2005). A network model of V1 with isotropic connectivity have been shown to exhibit orientation selectivity (Ernst et al., 2001). Based on these evidences, we suggest that our present model reproduces some of the basic properties of functionally organized biological neural networks such as V1. The dynamics of specific neural network architecture in the brain is to be studied on top of these basic findings.

Patchy activities are observed in physiological conditions (Tsodyks et al., 1999; Kenet et al., 2003). The transition of the patches to neighboring spaces observed in the simulation is consistent with the physiological data which suggest that the ongoing activities have a tendency to make transitions to the cortical areas representing neighboring angles (Kenet et al., 2003).

At present, the exact relation between the traveling wave measured in the cortical slices (Petersen et al., 2003; Sanchez-Vives and McCormick, 2000) and the switching of ongoing activities in V1 (Tsodyks et al., 1999; Kenet et al., 2003; Goldberg et al., 2004) is not known. In the model studies, if the network has no Mexican-hat type interaction, the transition velocity is known to depend on the transition from the down-state to the up-state (Compte et al., 2003; Bazhenov et al., 2002; Golomb and Ermentrout, 2001, 2002). We have shown here in a generic neural network model that when the network has a Mexican-hat type

interaction, the process of transition from the up-state to the down-state sets a limit to the transition velocity, as the patch cannot start to move if there is no synaptic depression (see Fig. 3(f), except for $P_v = 0$). There is no significant effect of noise from spontaneously firing neurons on the transition. The rate-limiting significance of the transition from the up-state to the down-state rather than that from the down-state to the up-state in determining the velocity of traveling waves is one of the novel aspects in the present model. In models based on the attractor hypothesis studied previously (e.g., Cai et al., 2005), the introduction of synaptic depression has not been shown to result in a significant effect. Hill and Tononi (2005) did not explicitly quantify the effect of synaptic depression on the traveling wave velocity of ongoing spontaneous activities. In our model, the decrease in synaptic current by the synaptic depression and the resulting breakdown of the up-states is instrumental in realizing the moving patches of activities, as bistability has been introduced in the membrane potential through intrinsic ion channels.

As already mentioned, the mechanism based on the “single-state” hypothesis has been suggested to account for the coherent ongoing activities observed in the primary visual cortex (Goldberg et al., 2004). In a model adapting this hypothesis, spontaneous ongoing activities are the results of the dynamics of a single background state, driven by the cortical noise. In a model based on the attractor-state hypothesis, on the other hand, the transition velocity of the patch is constrained by the process of termination of the up-state.

The synaptic depression and depolarization-dependent potassium channels are possible candidates to trigger the transitions from the up-states to the down-states, affecting the ongoing activities in differential manners. Parameter sets (2) and (3) in Fig. 3(h) suggest that the effect on the traveling velocity is greater in the case of depolarization-dependent potassium channels than synaptic depression. In addition, the introduction of depolarization-dependent potassium channels is found to interfere with the effect of synaptic depression. In the case of synaptic depression only (Fig. 3(f)), larger rates of synaptic depression lead to larger traveling velocities. In contrast, when the synaptic depression and depolarization-dependent potassium channels coexist, larger rates of synaptic depression lead to smaller values of traveling velocities (Fig. 3(g)). The reason is as follows. The potassium current I_{KNa} increases in proportion to the accumulated number of spikes of excitatory neurons. The synaptic depression effectively decreases the amplitude of presynaptic excitatory current in proportion to the accumulated number of spikes of excitatory presynaptic neurons. The introduction of synaptic depression makes the membrane potential and the number of spikes in the up-state lower because of a decreased influx of current, compared to the condition of no synaptic depression (Fig. 3(a-2) and (a-3)). A lower number of spikes per unit time leads to a lower rate of I_{KNa} , making it take longer to break the balance between excitatory and inhibitory currents in the membrane potential. As a result, the synaptic depression diminishes the effect of depolarization-dependent potassium channel, leading to lower traveling velocities.

There are some ways to test the validity of the current model. Because of the nature of transitions between the up-states and down-states in the attractor-state model described here, affecting the mechanism of termination of the up-states would lead to corresponding changes in transition velocities. This point could be checked by changing the parameter involved in synaptic depression. The application of 4-aminopyridine (4-AP) or a high concentration of Ca^{2+} is known to accelerate the short-term synaptic depression (Varela et al., 1997). Our model predicts that when the synaptic depression parameter P_v is decreased, the transition velocity increases in the coexistence of synaptic

depression and depolarization-dependent potassium channels (Fig. 3(g)), and decreases in the condition of synaptic depression only (Fig. 3(f)). If there is no change in the transition velocity corresponding to the modification of synaptic depression, there are two possible interpretations. The first is that the depolarization-dependent potassium channels rather than the synaptic depression are responsible for causing the transition (condition (2) in Fig. 3(h), with $P_v = 0$), in which case the attractor-state hypothesis would be maintained. The second is that mechanisms other than those based on the attractor-state hypothesis, e.g., the single-state hypothesis, or the intermittent desuppressed state (Cai et al., 2005) are relevant to the physiological condition, with the introduction of synaptic depression not affecting the transition velocities.

In conclusion, the results reported here shed a new light into the physiological basis of spontaneous neural activities in the cortex. The ongoing activities sustained by the internal dynamics leads to a larger degree of freedom for the configuration of the cortical network involved in various computations. The intrinsic ability of the local network to undergo transitions between multiple states on its own might have an important role in salient cognitive functions, e.g., the memory consolidation process during sleep (Huber et al., 2004; Stickgold et al., 2000). The results of our simulation, taken as a whole, suggest that parameters in the dynamics of the generic network needs to be fine-tuned in order to reproduce the observed behavior of the biological neural network. The circuits in the brain therefore is likely to be operating in a narrow domain in the relevant parameter space, giving important constraints on cortical dynamics.

Acknowledgments

We thank (in alphabetical order) Toru Aonishi, Koji Ito, Yoshihiro Miyake, Eizo Miyashita, Kiyohiko Nakamura, Fumihiko Taya, and Masayuki Yamamura for helpful discussions. We are grateful for two anonymous reviewers for their insightful comments on an earlier version of our paper.

Appendix A. Supplementary data

Supplementary data associated with this article can be found, in the online version, at doi:10.1016/j.neures.2009.02.011.

References

- Abbott, L.F., Varela, J.A., Sen, K., Nelson, S.B., 1997. Synaptic depression and cortical gain control. *Science* 275, 220–224.
- Arieli, A., Shoham, D., Hildesheim, R., Grinvald, A., 1995. Coherent spatiotemporal patterns of ongoing activity revealed by real-time optical imaging coupled with single-unit recording in the cat visual cortex. *J. Neurophysiol.* 73, 2072–2093.
- Arieli, A., Sterkin, A., Grinvald, A., Aertsen, A., 1996. Dynamics of ongoing activity: explanation of the large variability in evoked cortical responses. *Science* 273, 1868–1871.
- Bazhenov, M., Timofeev, I., Steriade, M., Sejnowski, T.J., 2002. Model of thalamocortical slow-wave sleep oscillations and transitions to activated States. *J. Neurosci.* 22, 8691–8704.
- Ben-Yishai, R., Bar-Or, R.L., Sompolinsky, H., 1995. Theory of orientation tuning in visual cortex. *Proc. Natl. Acad. Sci. U.S.A.* 92, 3844–3848.
- Cai, D., Rangan, A.V., McLaughlin, D.W., 2005. Architectural and synaptic mechanisms underlying coherent spontaneous activity in V1. *Proc. Natl. Acad. Sci. U.S.A.* 102, 5868–5873.
- Compte, A., Sanchez-Vives, M.V., McCormick, D.A., Wang, X.J., 2003. Cellular and network mechanisms of slow oscillatory activity (<1 Hz) and wave propagations in a cortical network model. *J. Neurophysiol.* 89, 2707–2725.
- Crook, J.M., Kisvarday, Z.F., Eysel, U.T., 1998. Evidence for a contribution of lateral inhibition to orientation tuning and direction selectivity in cat visual cortex: reversible inactivation of functionally characterized sites combined with neuroanatomical tracing techniques. *Eur. J. Neurosci.* 10, 2056–2075.
- Ernst, U., Pawelzik, K., Sahar-Pikelyny, C., Tsodyks, M., 2001. Intracortical origin of visual maps. *Nat. Neurosci.* 4, 431–436.
- Goldberg, J.A., Rokni, U., Sompolinsky, H., 2004. Patterns of ongoing activity and the functional architecture of the primary visual cortex. *Neuron* 42, 489–500.

- Golomb, D., Ermentrout, G.B., 2001. Bistability in pulse propagation in networks of excitatory and inhibitory populations. *Phys. Rev. Lett.* 86, 4179–4182.
- Golomb, D., Ermentrout, G.B., 2002. Slow excitation supports propagation of slow pulses in networks of excitatory and inhibitory populations. *Phys. Rev. E* 65, 061911.
- Hill, S., Tononi, G., 2005. Modeling sleep and wakefulness in the thalamocortical system. *J. Neurophysiol.* 93, 1671–1698.
- Huber, R., Ghilardi, M.F., Massimini, M., Tononi, G., 2004. Local sleep and learning. *Nature* 430, 78–81.
- Jahr, C.E., Stevens, C.F., 1990. Voltage dependence of NMDA-activated macroscopic conductances predicted by single-channel kinetics. *J. Neurosci.* 10, 3178–3182.
- Kenet, T., Bibitchkov, D., Tsodyks, M., Grinvald, A., Arieli, A., 2003. Spontaneously emerging cortical representations of visual attributes. *Nature* 425, 954–956.
- Marino, J., Schummers, J., Lyon, D.C., Schwabe, L., Beck, O., Wiesing, P., Obermayer, K., Sur, M., 2005. Invariant computations in local cortical networks with balanced excitation and inhibition. *Nat. Neurosci.* 8, 194–201.
- Maye, A., Hsieh, C., Sugihara, G., Brembs, B., 2007. Order in spontaneous behavior. *PLoS ONE* 2, e443. doi:10.1371/journal.pone.0000443.
- McCormick, D.A., 1992. Neurotransmitter actions in the thalamus and cerebral cortex and their role in neuromodulation of thalamocortical activity. *Prog. Neurobiol.* 39, 337–388.
- Petersen, C.C., Hahn, T.T., Mehta, M., Grinvald, A., Sakmann, B., 2003. Interaction of sensory responses with spontaneous depolarization in layer 2/3 barrel cortex. *Proc. Natl. Acad. Sci. U.S.A.* 100, 13638–13643.
- Raichle, M.E., MacLeod, A.M., Snyder, A.Z., Powers, W.J., Gusnard, D.A., Shulman, G.L., 2001. A default mode of brain function. *Proc. Natl. Acad. Sci. U.S.A.* 98, 676–682.
- Sanchez-Vives, M.V., McCormick, D.A., 2000. Cellular and network mechanisms of rhythmic recurrent activity in neocortex. *Nat. Neurosci.* 3, 1027–1034.
- Stickgold, R., James, L., Hobson, J.A., 2000. Visual discrimination learning requires sleep after training. *Nat. Neurosci.* 3, 1237–1238.
- Tsodyks, M., Markram, H., 1997. The neural code between neocortical pyramidal neurons depends on neurotransmitter. *Proc. Natl. Acad. Sci. U.S.A.* 94, 719–723.
- Tsodyks, M., Kenet, T., Grinvald, A., Arieli, A., 1999. Linking spontaneous activity of single cortical neurons and the underlying functional architecture. *Science* 286, 1943–1946.
- Varela, J.A., Sen, K., Gibson, J., Fost, J., Abbott, L.F., Nelson, S.B., 1997. A quantitative description of short-term plasticity at excitatory synapses in layer 2/3 of rat primary visual cortex. *J. Neurosci.* 17, 7926–7940.
- Vincent, J.L., Patel, G.H., Fox, M.D., Snyder, A.Z., Baker, J.T., Van Essen, D.C., Zempel, J.M., Snyder, L.H., Corbetta, M., Raichle, M.E., 2007. Intrinsic functional architecture in the anaesthetized monkey brain. *Nature* 447, 83–86.
- Wang, X.J., 1999. Synaptic basis of cortical persistent activity: the importance of NMDA receptors to working memory. *J. Neurosci.* 19, 9587–9603.